Static Blood Flow Autoregulation in the Optic Nerve Head in Normal and Experimental Glaucoma

Lin Wang, Claude F. Burgoyne, Grant Cull, Simon Thompson, and Brad Fortune

Devers Eye Institute, Legacy Research Institute, Portland, Oregon

Correspondence: Lin Wang, Devers Eye Institute, Legacy Health, 1225 NE 2nd Avenue, Portland, OR 97232; lwang@deverseye.org.

Submitted: December 5, 2013
Accepted: January 2, 2014

Citation: Wang L, Burgoyne CF, Cull G, Thompson S, Fortune B. Static blood flow autoregulation in the optic nerve head in normal and experimental glaucoma. *Invest Ophthalmol Vis Sci.* 2014;55:873–880. DOI:10.1167/iovs.13-13716

Purpose. To characterize the static blood flow autoregulation in the optic nerve head (ONH), and to investigate its role in hemodynamic changes in experimental glaucoma (EG).

Methods. Unilateral elevation of intraocular pressure (IOP) was induced in 15 adult rhesus macaques by laser treatment to the trabecular meshwork. Prior to and after laser treatment, retinal nerve fiber layer thickness (RNFLT) was assessed, biweekly, by spectral-domain optical coherence tomography. Optic nerve head static autoregulation was assessed by determining the percentage blood flow (BF) change after the IOP was acutely increased from 10 to 30, 40, or 50 mm Hg manometrically, utilizing a laser speckle flowgraphy device.

Results. Postlaser IOP (measured during average 7.7 ± 2.6 months) was 20.2 ± 5.9 mm Hg in EG eyes and 12.3 ± 2.6 mm Hg in control eyes ($P < 0.0001$). Retinal nerve fiber layer thickness was reduced by 33 ± 22% of the baseline values ($P < 0.001$) on average in EG eyes and by 0.4 ± 2.3% in control eyes ($P > 0.05$). The ONH BF remained at a constant level within a range of ocular perfusion pressure (OPP), 41 mm Hg and above. The autoregulation curves, created by all 723 tests in control and 352 tests in EG, were not significantly different ($P = 0.71$).

Conclusions. Optic nerve head BF in normal nonhuman primate (NHP) eyes is effectively regulated within a range of OPP approximately 41 mm Hg and above. Chronic IOP elevation causes no remarkable change to the static autoregulation within the ONH of EG eyes.

Keywords: autoregulation, intraocular pressure, ocular perfusion pressure, experimental glaucoma

Open angle glaucoma is an ocular disease characterized by progressive retinal ganglion cell death and axon loss, ultimately leading to irreversible visual field loss. Though elevated intraocular pressure (IOP) is still the only treatable risk factor for glaucoma, accumulating evidence suggests that blood flow (BF) in the optic nerve head (ONH) is compromised.[1–12] This hemodynamic alteration, including the observation in our recent studies in experimental glaucoma (EG),[13,14] has been proposed to play a role in the pathological processes of glaucomatous optic neuropathy, either directly or indirectly by increasing the susceptibility of the ONH to IOP.[15–18] One possible mechanism underlying this compromised BF in the ONH is autoregulation dysfunction.[16–23]

Autoregulation is an intrinsic ability of vascular beds, including ocular tissues, to maintain a constant level of BF in the face of perfusion pressure fluctuation and varied metabolic demand. The capacity of autoregulation may become less potent, or may completely fail, in glaucoma leading to the tissue's being underperfused[24] while greater diurnal IOP variations[25,26] and more pronounced reductions in nocturnal blood pressure occur.[27,28] Based upon the concept of autoregulation, a line of studies has examined the autoregulation capacity in glaucoma by determining the relative BF change in retina,[29,30] choroid,[31,32] and retrobulbar arteries[33–36] after either BP[29,37] or IOP[30,32] or blood carbon dioxide concentration[35,38] is artificially altered from an ambient level to another level. Although these studies suggest that BF autoregulation is altered in those tissues, to date, no clear evidence of autoregulation dysfunction has been demonstrated in the ONH,[32,37] the primary site of glaucomatous damage to the retinal ganglion cell axons.[39–41] These incomplete results hinder our understanding of the vascular role in glaucoma pathophysiology and are due, at least partially, to the methodological limits of how autoregulation is examined.

The common methodology used in the clinic to quantify autoregulation capacity is measurement of BF differences before and after the ocular perfusion pressure (OPP) is artificially increased or decreased. The normalized BF change thus represents the autoregulation capacity at a given OPP level tested. A series of such BF changes in response to OPP changes, over a wide range of OPP, constitutes a classic autoregulation curve or pressure–flow (P-F) relationship (see Fig. 1).[42] This curve includes a plateau across the range of OPP where the BF is fully compensated by autoregulation. When the OPP fluctuations exceed the critical range defined by this plateau, that is, beyond the lower and upper limits of the autoregulation range (LLA and ULA, respectively), vasomotor adjustments are incomplete and BF will gradually decrease or increase passively as OPP changes. In this study, the P-F relationships within these ranges of OPP are referred to as "lower slope" and "upper slope" (Fig. 1).

When autoregulation capacity is assessed in glaucoma, BF is often measured at a given level of OPP chosen depending on the manner in which the OPP is challenged, for example, by increasing the blood pressure or by altering IOP. It is assumed that any BF abnormality at a measured OPP represents the

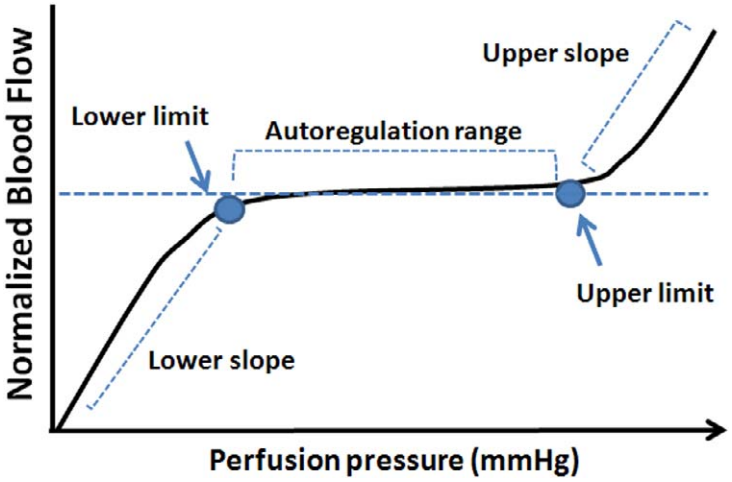

FIGURE 1. A schematic showing an autoregulation curve that describes the relationship between BF and perfusion pressure.

autoregulation status in glaucoma. However, according to studies in cerebral circulation, autoregulation may change differently depending upon the disease. For example, the autoregulatory curve may shift toward the higher OPP in chronic hypertension[24]; in ischemic cerebrovascular diseases, a loss of autoregulation could be simply attributed to an alteration within the lower slope of OPP,[43] while the normal plateau can be absent in diabetes.[44] Because the autoregulation curve changes within glaucoma are still unknown, the BF change measured at a given OPP may not represent the exact autoregulation status. This is a likely source of discrepancy between the studies in which autoregulation capacity is examined at different OPPs. However, to construct a complete autoregulation curve covering a full range of OPP is difficult, if not impossible, in a clinical setting.

The nonhuman primate (NHP) EG model with chronic IOP elevation has been used to study ONH BF.[14,45] In our previous studies using this model, ONH BF in the EG eye has been found to be significantly lower than in the control eye when the BF was measured at a reduced OPP by increasing the IOP to 40 mm Hg.[14] In these eyes, the basal ONH BF (i.e., under manometric IOP control at 10 mm Hg) changes in a biphasic manner over the course of longitudinal follow-up through stages of EG: ONH BF is slightly increased during the early stage and then undergoes a continuous decline through later stages of EG.[13,14] This altered ONH BF observed under manometric IOP control at both normal and raised IOP suggests that ONH autoregulation is likely interrupted after a period of chronic IOP elevation in EG and progresses secondary to the continuous optic neuronal degeneration.

In the current study on this cohort of NHP EG, we tested an assumption that chronic IOP elevation results in autoregulation impairment, which is associated with the reduced ONH BF demonstrated in our previous studies.[13,14] This was achieved by comparing the autoregulation curve between EG and normal control eyes. The autoregulation curve was created based on a series of relative ONH BF changes, each measured in response to an acute OPP decrease induced by instantaneous IOP elevation monitored across stages of EG. In addition to the comparison of the whole autoregulation curve between the study eye groups, parameters that characterize the autoregulation curve, including the lower slope, LLA, and plateau (see Fig. 1), were compared for individual animals (pairs of eyes) as well. Although the experimental model precludes a scenario whereby vascular dysregulation could serve as a primary insult in glaucomatous damage,[46] the results for the first time reveal a general pattern for an autoregulation curve within the ONH after chronic IOP elevation. Since the BF was measured after it reached a steady state post-OPP challenge, these measurements represent so-called static autoregulation, in contrast to "dynamic autoregulation" that describes the rapid, continuous course of BF response during an OPP challenge,[47,48] which will be reported separately.

METHODS

Animals and Anesthesia

Fifteen adult rhesus monkeys (*Macaca mulatta*) were included in the study, 14 females and 1 male. Their average age at the beginning of the study (±SD) was 9.0 ± 2.6 years (range, 5–14 years), and average weight was 6.4 ± 1.7 kg. In all cases, anesthesia was induced with intramuscular ketamine (15 mg/kg; Henry Schein Animal Health, Dublin, OH) and xylazine (1.5 mg/kg; Akorn, Inc., Decatur, IL), along with a single subcutaneous injection of atropine sulfate (0.05 mg/kg; Butler Schein Animal Health, Dublin, OH). Animals were then intubated and breathed air plus 10% oxygen spontaneously. Heart rate, end tidal CO_2, and arterial oxygenation saturation were monitored continuously. Body temperature was maintained with a heating pad at 37°C. Pupils were fully dilated with 1.0% tropicamide (Alcon Laboratories, Inc., Fort Worth, TX). One of the superficial branches of a tibial artery was cannulated with a 27-gauge needle, which was connected to a pressure transducer (BLPR2; World Precision Instruments, Sarasota, FL) and a four-channel amplifier system (Lab-Trax-4/24T; World Precision Instruments) for continuous arterial blood pressure (BP) recording. Anesthesia was maintained by continuous administration of pentobarbital (8–12 mg/kg/h, intravenous) using an infusion pump (Aladdin; World Science Instruments, Inc., Sarasota, FL) for all procedures except during trabecular meshwork laser sessions. All procedures were performed with the animals under general anesthesia, adhering to the ARVO Statement for the Use of Animals in Ophthalmic and Vision Research, and were approved and monitored by the Institutional Animal Care and Use Committee at Legacy Research Institute.

Retinal Nerve Fiber Layer Thickness Measurement

The progression of structural damage during the development of EG was monitored by longitudinal measurements of peripapillary retinal nerve fiber layer thickness (RNFLT) in

both eyes of each animal using a spectral-domain optical coherence tomography (SD-OCT) instrument (Spectralis; Heidelberg Engineering GmbH, Heidelberg, Germany). For each measurement, a single circular B-scan (12° diameter) was performed; 9 to 16 individual sweeps were averaged to comprise a final B-scan at each session. The automated layer segmentations generated by the instrument were manually corrected when the algorithm had obviously erred during delineation of the RNFL inner and outer borders. Spectral-domain OCT data were exported for extraction of RNFLT values by custom software.[49]

Induction of Chronic Unilateral Experimental IOP Elevation

Laser treatment to one eye of each animal was performed under ketamine and xylazine anesthesia. One hundred eighty degrees of the trabecular meshwork (50-μm spot size, 1.0-second duration, 600–750 mW power) was treated in each of two separate sessions at least 2 weeks apart. After each treatment, a sub-Tenon's injection of 0.5 mL dexamethasone (10 mg/mL; APP Pharmaceuticals LLC, Shaumberg, IL) was given in the inferior fornix of the treated eye. Laser treatments were repeated (but limited to a 45° or 90° sector) on subsequent occasions as necessary to achieve sustained IOP elevation.

IOP Measurement

Intraocular pressure was measured at each test session by rebound tonometry (Tonopen XL; Reichert, Inc., Depew, NY) in both eyes of each animal (a mean of three measurements per eye) within 30 minutes of general anesthesia induction. After the initial IOP measurements, IOP was set in both eyes manometrically to 10 mm Hg. Two 27-gauge needles were inserted into the anterior chamber of each eye. One needle was connected to a manometer set at 10 mm Hg; the other was connected to a pressure transducer to record actual eye pressure as previously described.[13]

Blood Flow Measurement With Laser Speckle Flowgraphy

The laser speckle flowgraphy (LSFG) technique (Softcare; Iizuka, Japan) was used to measure BF in the NHP ONH and has been described in detail within previous publications.[14,50,51] In brief, a fundus camera equipped within the LSFG device was focused on an area centered on the ONH. The area is approximately 3.8 × 3 mm (width × height). After the laser is switched on ($\lambda = 830$ nm, maximum output power, 1.2 mW), a speckle pattern is generated due to random interference of the scattered light from the illuminated tissue area. The speckle pattern is continuously imaged by a charge-coupled device (700 × 480 pixels) at a frequency of 30 frames per second for 4 seconds at a time.

Offline analysis software (LSFG Analysis; Softcare) computed mean blur rate (MBR) of the speckle images. Mean blur rate is a squared ratio of mean intensity to the standard deviation of light intensity of the image, which varies temporally and spatially according to the velocity of blood cell movement and correlates well with capillary BF within the ONH validated by the microsphere[14] and the hydrogen clearance methods.[52] Thus, the MBR has been used as a BF index. A composite MBR map representing BF distribution within the ONH disc was generated from the images of each 4-second series. After eliminating the area corresponding to large blood vessels within the images, capillary BF within the remaining ONH disc area was averaged and reported in arbitrary units (AU) of MBR.

Quantification of Static Blood Flow Autoregulation

For each measurement of static BF autoregulation, the IOP in the test eye was manometrically set at 10 mm Hg and left to equilibrate for at least 5 minutes. With all vital signs (oxygen saturation, heart rate, and end tidal CO_2) stabilized, baseline BF (MBR) was measured with the LSFG for 4 seconds. The saline reservoir was then switched to a height calibrated to be equivalent to 30, 40, or 50 mm Hg and kept at the higher level for at least 3 minutes. After the BF was measured again for another 4 seconds, the reservoir was returned to the previous level (10 mm Hg). The percentage BF change measured at each acutely elevated IOP level relative to that measured at an IOP of 10 mm Hg was calculated. During each test session, the above measurement protocol was repeated for all three levels of acute IOP elevation. A series of the relative ONH BF changes measured at different OPP levels during multiple test sessions was used to create autoregulation curves for both EG and control eyes.

The OPP was estimated by subtracting the IOP from the recorded mean arterial BP (diastolic pressure + one-third of pulse pressure) and an additional 5 mm Hg to account for the height difference between the eye and the artery where BP was recorded.

Experimental Design

For each animal, three to five prelaser baseline sessions were included to establish baseline values of IOP, RNFLT, and ONH autoregulation in each eye. Then chronic IOP elevation was initiated by laser treatment in one eye of each animal. Thereafter, the same measurements were repeated once every 2 weeks for the duration of the postlaser follow-up. Most animals (9 of 15) were followed until a relatively advanced stage, when RNFLT in the EG eye was reduced by more than 35% of its prelaser baseline value. Six of the 15 animals were followed only during an earlier stage of EG, then killed in order to evaluate histological and molecular changes in early EG eyes. In these animals, the average RNFLT was reduced by less than 10%, on average. At the end of each experiment, the animals were killed humanely under deep anesthesia for histopathological studies.

Data Analysis and Statistics

The relative ONH BF changes obtained at different OPPs were fitted with segmental linear regression to determine three parameters: the lower slope, LLA, and plateau (Prism 6.03; GraphPad Software, Inc., La Jolla, CA). The difference between autoregulation curves of the EG eye and control eye was evaluated with a mixed model of covariance analysis (ANCOVA) using the Satterthwaite method for control of random effect (Statistica 12; StatSoft, Inc., Tulsa, OK). All IOP, RNFLT, and BF were reported as an average ± standard deviation (SD) unless otherwise specified. Mean difference of the measurements was evaluated by Student's *t*-test after the data were confirmed to have normal distribution.

Results

Intraocular Pressure and RNFLT

Within the baseline testing sessions, there was no difference between the two eyes for mean IOP (14.1 ± 2.1 vs. 13.8 ± 2.3, $P = 0.28$). Postlaser IOP in the EG eyes was significantly

Investigative Ophthalmology & Visual Science

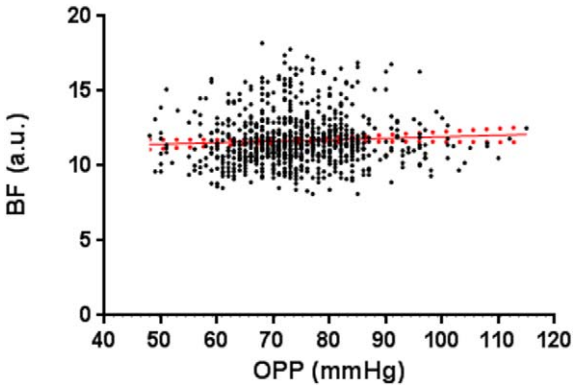

FIGURE 2. Optic nerve head BF (AU) measured at different OPPs when the IOP was controlled manometrically at 10 mm Hg in all eyes without laser treatment and all eyes before laser treatment. Note that the lowest OPP was 48 mm Hg, which is higher than the LLA shown in Figure 3. A linear regression was fitted for all the data ($Y = 0.01 \times X + 10.94$, $R^2 = 0.003$; *red dotted lines*: standard error).

increased compared with that in the control eyes (20.2 ± 5.9 vs. 12.3 ± 2.6 mm Hg, respectively ($P < 0.0001$). Peak IOP was 42.2 ± 10.2 mm Hg for EG eyes and 18.9 ± 2.8 mm Hg for control eyes. The average duration of postlaser treatment was 7.7 ± 2.6 months (ranging from 3.6 to 12.5 months). The average values for RNFLT in the control eyes at the end of longitudinal follow-up were –0.4% ± 2.3% relative to baseline (ranging from –6.2% to +4.3%). The average RNFLT in the EG eyes at the end of the experiment was –33 ± 22% relative to baseline values ($P < 0.001$). In the six animals followed only to an earlier stage of EG, the average RNFL loss was 9 ± 8% below baseline (ranging from 3.5% above to 17.1% below baseline) in the EG eyes. The nine advanced EG eyes had RNFLT loss of 46 ± 11%, ranging from 36% to 62%).

ONH BF Autoregulation in Control Eyes

To describe the P-F relationship within the range of ambient OPP, or ONH autoregulation curve, all the tests ($n = 723$) from eyes without laser treatment (contralateral control, $n = 15$ eyes) and the designated EG eyes before any laser treatment ("prelaser," $n = 15$) were included for the analysis. This analysis aims to determine the range of OPP within which the

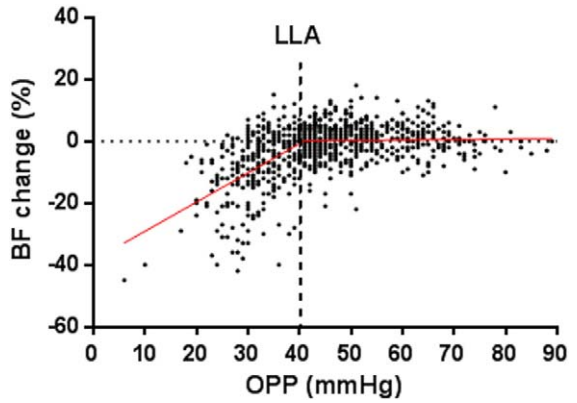

FIGURE 3. The relative ONH BF change (%) after the OPP was reduced by increasing the IOP in the normal control eyes ($n = 723$ tests). The *solid red lines* are two regression lines fitted by segmental linear regression, representing the lower slope and the plateau. The *red dotted lines* are standard errors. The LLA (40.7 mm Hg) is marked with a *vertical blue dotted line*.

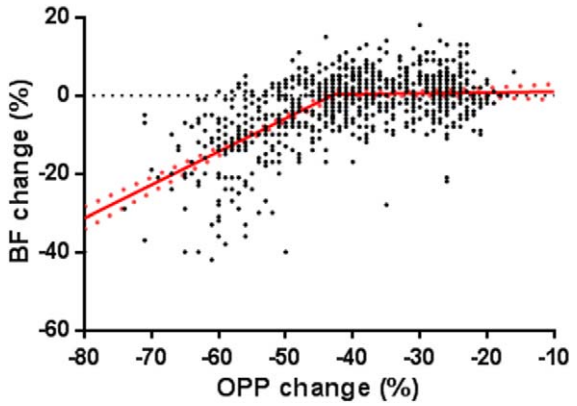

FIGURE 4. Blood flow change (%) is plotted against the percentage OPP decrease induced by manometrical IOP increase within each test. The data were fitted with a segmental linear regression. The intersection of the two regression lines (–43%) indicates the percentage of OPP change from which the BF started to decline. *Red dotted lines*: standard error.

ONH BF remains relatively stable. As shown in Figure 2, the ONH BF (AU) was measured at OPPs from 48 to 115 mm Hg. Since the IOPs during the BF measurements were all set at 10 mm Hg, the varied OPP resulted from the difference of BP between animals and between longitudinal tests. Analysis of a linear regression showed that the ONH BF within the range of OPP did not correlate ($R^2 = 0.003$).

Figure 3 shows the percentage ONH BF change from each of the test dates in Figure 2 after the IOP was acutely increased from 10 to 30, 40, or 50 mm Hg. This analysis aims to establish an additional portion of the autoregulation curve, specifically to determine the LLA (OPP from where BF starts to decline) and to characterize the lower slope. As shown, a segmental linear regression generated two distinguishable regression lines. The LLA was defined as the intersection of the two regression lines, which was approximately 40.7 mm Hg OPP (95% confidence limit (CL): 38.81–42.52). The ONH BF changed little (plateau) if the resultant OPP was above the LLA, but the BF started to decline (lower slope) once the OPP was below the LLA. The intercept of the lower slope was –39%.

In Figure 4, the same BF data in Figure 3 are plotted against percentage OPP change; that is, the relative decrease of OPP (%) resulted from the acute IOP increase from 10 to 30, 40, and 50 mm Hg. Segmental linear regression analysis showed that the BF started to decline when the OPP decreased more than 43%.

ONH BF Autoregulation in EG Eyes

Comparison of Autoregulation Curves Between EG and Control Eyes. In this analysis, the ONH BF changes (%) in response to the acute OPP decrease in all postlaser tests ($n = 352$) in EG eyes were pooled together to construct an autoregulation curve. This curve was then compared with that derived from control eyes ($n = 723$ tests) in Figure 3. The reason for pooling all the tests together was to enhance the statistical power. However, since RNFLT loss progressed more slowly in some animals, the results may be biased toward those animals with a greater number of tests. This random effect was controlled by the Satterthwaite method while a mixed model of ANCOVA was used to test the difference between EG and control eyes. The result showed no difference between the two groups of eyes ($P = 0.71$), although the lower slope and the plateau showed a tendency toward a slightly greater BF

Investigative Ophthalmology & Visual Science

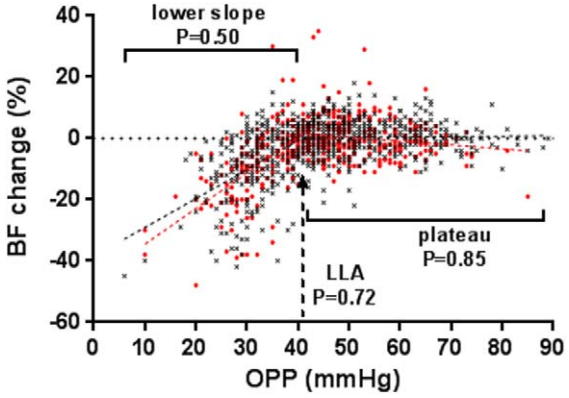

Figure 5. Comparison of the ONH BF autoregulation curve between control (*black*) and EG (*red*) eyes ($n = 15$ eyes for each). The total numbers of tests were 723 for control eyes and 352 for EG eyes. Analysis with a mixed model of ANCOVA showed no difference between EG and the control eyes ($P = 0.71$). The probabilities that the lower slope, LLA, and plateau were the same between the two eyes are marked correspondingly in the graph.

decrease in EG eyes. A further comparison specifically for the lower slope, LLA, and the plateau showed no remarkable difference between the two groups of eyes as well ($P = 0.50$, $P = 0.72$, and $P = 0.85$, respectively; see Fig. 5).

Since the BF changes in EG eyes were collected throughout the experiment after laser treatment, pooling all the data, including the early stage, could potentially mask a possible ONH autoregulation change. Therefore, the above analysis was repeated in two subdivided groups, (1) earlier-stage EG ($n = 15$ eyes), in which RNFLT loss was less than 20%, and (2) advanced EG eyes ($n = 9$ eyes), in which RNFLT loss was more than 20%. Thereby, the autoregulation curve representing each subgroup was compared with the control eyes for the whole curve, the slope, and the plateau. The results showed that none of the parameters or LLA in the EG eye was significantly different compared with normal control eyes (Fig. 6, Table).

Comparison of the Autoregulation Curve Between Individual EG Eye and Pooled Controls or the Contralateral Control Eye. In the previous analyses, the BF measurements in the EG and control eyes were pooled together to generate the autoregulation curves. Although the approach enhanced the overall statistical power, it might have overlooked the individual eyes with possible autoregulation changes. Therefore, in this analysis the autoregulation curve from each EG eye was compared with either pooled controls or the contralateral control eye. Three animals were excluded due to too few data points on the lower slope (0–2) to perform the analysis. The results demonstrate no significant difference between each EG eye and pooled control eyes or their own contralateral control eye (data not shown).

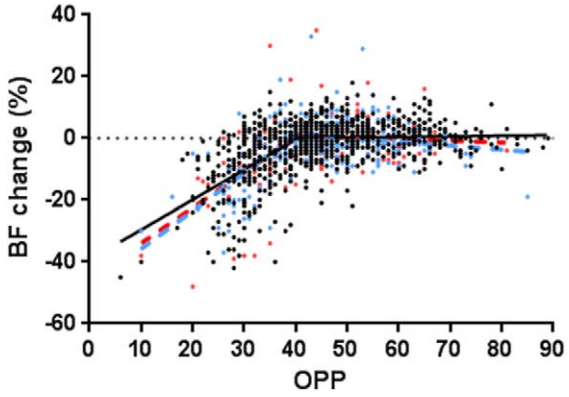

Figure 6. The ONH autoregulation curves in early EG eyes (*blue*; $n = 297$ tests from 15 eyes), advanced EG eyes (*red*; $n = 132$ tests from 9 eyes), and all control eyes (*black*). The data from each group were fitted with a segmental linear regression model.

Table. Probability That the Autoregulation Curve and Corresponding Parameters in Early and Advanced EG Eyes Were the Same as in Control Eyes

	Whole Curve*	Lower Slope†	LLA†	Plateau†
Early EG	$P = 0.48$	$P = 0.22$	$P = 0.53$	$P = 0.74$
Advanced EG	$P = 0.85$	$P = 0.95$	$P = 0.40$	$P = 0.89$

* Mixed model of ANCOVA.
† Segmental linear regression model.

Discussion

To test the prediction that chronic IOP elevation impairs ONH static autoregulation capacity in this NHP glaucoma model, the ONH BF autoregulation curve was created from BF responses across a wide range of OPP and compared between EG eyes and control eyes. The results showed that within the ONH of the control eyes, BF was effectively regulated within the OPP range from 41 to 115 mm Hg. Conversely, when the OPP was below 41 mm Hg, the BF declined linearly with OPP. In the EG eyes, the autoregulation curve and the corresponding parameters showed no significant difference from the control eyes, regardless of whether the comparison was made between pooled data or individual animals.

An important parameter measuring the autoregulation efficacy is the critical OPP point (LLA), from where and below the BF starts to decline. Previous studies investigating the ONH autoregulation showed that LLA varied in a wide range, within and between species, from 20 to 48 mm Hg[53,54] in cats and 30 mm Hg in monkeys.[55] In humans, the LLA was estimated to be between 10 and 26,[56] 22,[57] or 39 mm Hg[58] based on the BP and IOP provided in the papers. In these studies the critical point at which BF started to decline was expressed by percentage OPP change; this corresponding critical point was 20%,[59] 40%,[60] or 60%[57,61] OPP decrease from an ambient level.[57,61] In the current study in NHP ONH, the BF started to decline from OPP 41 mm Hg (Fig. 3), or 43% if the OPP change was expressed by a percentage decrease (Fig. 4).

Besides the difference in species, BF measurement methodology, speed of OPP change,[57] and individual variation,[57,59] the approach to determining the LLA may account for the differences of the measured LLA. To define a LLA often requires identifying an OPP level below which the BF decreases significantly. In studies with a smaller sample size and larger measurement variation, this BF level is often found at a much lower OPP compared to that in a study with a larger sample size and smaller measurement variation. In the current study, the LLA was estimated by determining the intersection of two regression lines generated by a segmental linear regression model, which defines the LLA as an OPP where the BF just begins to decline.

A previous study on this same cohort of NHP glaucomatous animals[62] showed that beyond approximately 10% of RNFLT loss, the ONH BF in EG eyes progressively declined to more than 20% below the baseline value, and the decrease was

correlated closely with the loss of RNFLT. It was proposed in that study that this reduced BF was at least partially a result of reduced metabolic demand after retinal ganglion axon loss and/or possibly a result of autoregulation dysfunction. In the current study, when the P-F relationship was described based upon static BF autoregulation and compared between EG and control eyes, it failed to show any significant difference in static autoregulation. Thus, it seems that at least in these chronic IOP-induced EG eyes, the static autoregulation is not a predominant factor accounting for the reduced ONH BF observed in the previous study.[62]

There are additional factors that should be considered regarding this insignificant autoregulation difference. First, in this NHP EG model, the ONH BF in the prelamina and lamina region during the early stage was in fact increased.[62] In a subgroup of these experiments, the increased BF was also observed during the later stages within the retrolaminar region.[14] These findings agree with earlier studies in the same NHP EG model, which showed both increased and decreased ONH BF[45] and upregulated retinal BF in the early stages of human glaucoma.[63] On the one hand, this strongly suggests autoregulation dysfunction occurring in glaucoma; on the other hand, the up- and downregulated BF change may obscure the observation of a potential autoregulation change in the ONH. More importantly, the different sensitivities of autoregulation components should also be taken into account. As mentioned previously, static and dynamic aspects are two related but different components during the process of autoregulation. Studies in the brain have shown that each component may represent different mechanisms.[64] Under certain diseased conditions, such as acute ischemic stroke and brain injuries, the impairment to these two components has been demonstrated to be disassociated.[65,66] One additional factor that likely contributes to the insignificant change observed here for static autoregulation is the wide variation of ONH BF response to the acute IOP increase in both control and EG eyes (see Fig. 3). This large variation has been observed in the human ONH as well. In those studies, after the IOP was acutely increased by a negative pressure suction cup on the sclera, the ONH BF reduction varied between approximately 15%[59] and >50%[57] (estimates based on the data provided in these previous reports). Thus, this variation is likely one of the sources of variability in the detection of autoregulation changes in both human glaucoma and this EG model.

Several limitations are associated with this study. As has been detailed in previous reports, the LSFG, like most other optically based techniques, has limited tissue penetration in addition to the inherent calibration error between in vitro and in vivo measurements.[14,51,62] The BF measured by the LSFG derives largely from the anterior portion of the optic nerve and to a certain degree underestimates true BF. This is also part of the reason for the higher intercept in normal eyes (–39% at OPP = 0), although a nonzero BF intercept is possible at "zero" OPP because the systolic arterial pressure can be ~30 mm Hg above mean arterial pressure[67] used for the calculation of OPP. It should also be noted that the present study was conducted in anesthetized animals. Even though the anesthetics were carefully selected to minimize the inhibitory effect upon autoregulation during the tests, caution is warranted in comparing the results with human subjects. In addition, chronic IOP elevation and the course of EG in NHP eyes are still relatively rapid compared to observations in human glaucoma because peak IOP in the EG eyes was probably higher than most treated human glaucoma and damage developed in mere months. It is possible that the ONH autoregulation system is still functionally intact despite loss of neuronal tissue (i.e., RNFLT loss).

In summary, the current study demonstrated, first, that the normal ONH in NHP has a strong autoregulation capability to maintain a constant BF within the OPP range from 41 mm Hg and above. Secondly, it showed that chronic IOP elevation causes no remarkable autoregulation change in the ONH of EG eyes when examined by the static component. Thirdly, although the results may support our previous premise that reduced ONH BF in the EG eye is largely a result of reduced metabolic demand after neuronal tissue loss, continuing investigation utilizing different approaches, specifically examining the dynamic autoregulation component within the ONH of these same EG animals, is necessary. A parallel report on this series of studies will describe the details of dynamic autoregulation in the ONH of this EG model.

Acknowledgments

The authors thank Chelsea Piper for her technical assistance, Manoj Pathak for consultation on the statistical analysis, and Leo Schmetterer for valuable comments.

Supported by National Institutes of Health Grant R01-EY019939 and Legacy Good Samaritan Foundation, Portland, Oregon.

Disclosure: **L. Wang**, None; **C.F. Burgoyne**, None; **G. Cull**, None; **S. Thompson**, None; **B. Fortune**, None

References

1. Jia YL, Morrison JC, Tokayer J, et al. Quantitative OCT angiography of optic nerve head blood flow. *Biomed Opt Express*. 2012;3:3127–3137.
2. Yokoyama Y, Aizawa N, Chiba N, et al. Significant correlations between optic nerve head microcirculation and visual field defects and nerve fiber layer loss in glaucoma patients with myopic glaucomatous disk. *Clin Ophthalmol*. 2011;5:1721–1727.
3. Sugiyama T, Shibata M, Kojima S, Ikeda T. Optic nerve head blood flow in glaucoma. In: Kubena T, ed. *Mystery of Glaucoma*. New York: InTech; 2011:207–218.
4. Chiba N, Omodaka K, Yokoyama Y, et al. Association between optic nerve blood flow and objective examinations in glaucoma patients with generalized enlargement disc type. *Clin Ophthalmol*. 2011;5:1549–1556.
5. Sato EA, Ohtake Y, Shinoda K, Mashima Y, Kimura I. Decreased blood flow at neuroretinal rim of optic nerve head corresponds with visual field deficit in eyes with normal tension glaucoma. *Graefes Arch Clin Exp Ophthalmol*. 2006;244:795–801.
6. Hafez AS, Bizzarro RL, Lesk MR. Evaluation of optic nerve head and peripapillary retinal blood flow in glaucoma patients, ocular hypertensives, and normal subjects. *Am J Ophthalmol*. 2003;136:1022–1031.
7. Piltz-Seymour JR, Grunwald JE, Hariprasad SM, Dupont J. Optic nerve blood flow is diminished in eyes of primary open-angle glaucoma suspects. *Am J Ophthalmol*. 2001;132:63–69.
8. Findl O, Rainer G, Dallinger S, et al. Assessment of optic disk blood flow in patients with open-angle glaucoma. *Am J Ophthalmol*. 2000;130:589–596.
9. Kerr J, Nelson P, O'Brien C. A comparison of ocular blood flow in untreated primary open-angle glaucoma and ocular hypertension. *Am J Ophthalmol*. 1998;126:42–51.
10. Michelson G, Schmauss B, Langhans MJ, Harazny J, Groh MJ. Principle, validity, and reliability of scanning laser Doppler flowmetry. *J Glaucoma*. 1996;5:99–105.
11. Michelson G, Langhans MJ, Groh MJ. Perfusion of the juxtapapillary retina and the neuroretinal rim area in primary open angle glaucoma. *J Glaucoma*. 1996;5:91–98.

12. Hamard P, Hamard H, Dufaux J, Quesnot S. Optic nerve head blood flow using a laser Doppler velocimeter and haemorheology in primary open angle glaucoma and normal pressure glaucoma. *Br J Ophthalmol*. 1994;78:449–453.
13. Cull G, Burgoyne CF, Fortune B, Wang L. Longitudinal hemodynamic changes within the optic nerve head in experimental glaucoma. *Invest Ophthalmol Vis Sci*. 2013;54:4271–4277.
14. Wang L, Cull GA, Piper C, Burgoyne CF, Fortune B. Anterior and posterior optic nerve head blood flow in nonhuman primate experimental glaucoma model measured by laser speckle imaging technique and microsphere method. *Invest Ophthalmol Vis Sci*. 2012;53:8303–8309.
15. Maumenee AE. Causes of optic nerve damage in glaucoma. Robert N. Shaffer lecture. *Ophthalmology*. 1983;90:741–752.
16. Flammer J, Orgul S, Costa VP, et al. The impact of ocular blood flow in glaucoma. *Prog Retin Eye Res*. 2002;21:359–393.
17. Hayreh SS. The 1994 Von Sallman Lecture. The optic nerve head circulation in health and disease. *Exp Eye Res*. 1995;61:259–272.
18. Anderson DR. Introductory comments on blood flow autoregulation in the optic nerve head and vascular risk factors in glaucoma. *Surv Ophthalmol*. 1999;43(suppl 1):S5–S9.
19. Spaeth GL. Fluorescein angiography: its contributions towards understanding the mechanisms of visual loss in glaucoma. *Trans Am Ophthalmol Soc*. 1975;73:491–553.
20. Harris A. *Ocular Blood Flow in Glaucoma: Myths and Reality*. Amsterdam: Kugler Publications; 2009; 18–19.
21. Venkataraman ST, Flanagan JG, Hudson C. Vascular reactivity of optic nerve head and retinal blood vessels in glaucoma—a review. *Microcirculation*. 2010;17:568–581.
22. Schmidl D, Garhofer G, Schmetterer L. The complex interaction between ocular perfusion pressure and ocular blood flow—relevance for glaucoma. *Exp Eye Res*. 2010;93:141–155.
23. James B. Blood flow in the pathogenesis of glaucoma. *Curr Opin Ophthalmol*. 1993;4:65–72.
24. Vavilala MS, Lee LA, Lam AM. Cerebral blood flow and vascular physiology. *Anesthesiol Clin North America*. 2002;20:247–264.
25. Wilensky JT. The role of diurnal pressure measurements in the management of open angle glaucoma. *Curr Opin Ophthalmol*. 2004;15:90–92.
26. Choi J, Kim KH, Jeong J, Cho HS, Lee CH, Kook MS. Circadian fluctuation of mean ocular perfusion pressure is a consistent risk factor for normal-tension glaucoma. *Invest Ophthalmol Vis Sci*. 2007;48:104–111.
27. Leske MC. Ocular perfusion pressure and glaucoma: clinical trial and epidemiologic findings. *Curr Opin Ophthalmol*. 2009;20:73–78.
28. Costa VP, Arcieri ES, Harris A. Blood pressure and glaucoma. *Br J Ophthalmol*. 2009;93:1276–1282.
29. Feke GT, Pasquale LR. Retinal blood flow response to posture change in glaucoma patients compared with healthy subjects. *Ophthalmology*. 2008;115:246–252.
30. Nagel E, Vilser W, Lanzl IM. Retinal vessel reaction to short-term IOP elevation in ocular hypertensive and glaucoma patients. *Eur J Ophthalmol*. 2001;11:338–344.
31. Ulrich A, Ulrich C, Barth T, Ulrich WD. Detection of disturbed autoregulation of the peripapillary choroid in primary open angle glaucoma. *Ophthalmic Surg Lasers*. 1996;27:746–757.
32. Weigert G, Findl O, Luksch A, et al. Effects of moderate changes in intraocular pressure on ocular hemodynamics in patients with primary open-angle glaucoma and healthy controls. *Ophthalmology*. 2005;112:1337–1342.
33. Evans DW, Harris A, Garrett M, Chung HS, Kagemann L. Glaucoma patients demonstrate faulty autoregulation of ocular blood flow during posture change. *Br J Ophthalmol*. 1999;83:809–813.
34. Gherghel D, Orgul S, Gugleta K, Gekkieva M, Flammer J. Relationship between ocular perfusion pressure and retrobulbar blood flow in patients with glaucoma with progressive damage. *Am J Ophthalmol*. 2000;130:597–605.
35. Harris A, Sergott RC, Spaeth GL, Katz JL, Shoemaker JA, Martin BJ. Color Doppler analysis of ocular vessel blood velocity in normal-tension glaucoma. *Am J Ophthalmol*. 1994;118:642–649.
36. Liu CJ, Chou YH, Chou JC, Chiou HJ, Chiang SC, Liu JH. Retrobulbar haemodynamic changes studied by colour Doppler imaging in glaucoma. *Eye*. 1997;11:818–826.
37. Pournaras CJ, Riva CE, Bresson-Dumont H, De Gottrau P, Bechetoille A. Regulation of optic nerve head blood flow in normal tension glaucoma patients. *Eur J Ophthalmol*. 2004;14:226–235.
38. Hosking SL, Harris A, Chung HS, et al. Ocular haemodynamic responses to induced hypercapnia and hyperoxia in glaucoma. *Br J Ophthalmol*. 2004;88:406–411.
39. Hayreh SS. Blood supply of the optic nerve head and its role in optic atrophy, glaucoma, and oedema of the optic disc. *Br J Ophthalmol*. 1969;53:721–748.
40. Burgoyne CF, Downs JC, Bellezza AJ, Suh JK, Hart RT. The optic nerve head as a biomechanical structure: a new paradigm for understanding the role of IOP-related stress and strain in the pathophysiology of glaucomatous optic nerve head damage. *Prog Retin Eye Res*. 2005;24:39–73.
41. Quigley HA, Addicks EM, Green WR, Maumenee AE. Optic nerve damage in human glaucoma. II. The site of injury and susceptibility to damage. *Arch Ophthalmol*. 1981;99:635–649.
42. Bill A, Sperber GO. Aspects of oxygen and glucose consumption in the retina: effects of high intraocular pressure and light. *Graefes Arch Clin Exp Ophthalmol*. 1990;228:124–127.
43. Paulson OB, Strandgaard S, Edvinsson L. Cerebral autoregulation. *Cerebrovasc Brain Metab Rev*. 1990;2:161–192.
44. Kastrup J, Norgaard T, Parving HH, Henriksen O, Lassen NA. Impaired autoregulation of blood flow in subcutaneous tissue of long-term type 1 (insulin-dependent) diabetic patients with microangiopathy: an index of arteriolar dysfunction. *Diabetologia*. 1985;28:711–717.
45. Quigley HA, Hohman RM, Sanchez R, Addicks EM. Optic nerve head blood flow in chronic experimental glaucoma. *Arch Ophthalmol*. 1985;103:956–962.
46. Flammer J, Konieczka K, Flammer AJ. The primary vascular dysregulation syndrome: implications for eye diseases. *EPMA J*. 2013;4:14.
47. Liang Y, Fortune B, Cull G, Cioffi GA, Wang L. Quantification of dynamic blood flow autoregulation in optic nerve head of rhesus monkeys. *Exp Eye Res*. 2010;90:203–209.
48. Tiecks FP, Lam AM, Aaslid R, Newell DW. Comparison of static and dynamic cerebral autoregulation measurements. *Stroke*. 1995;26:1014–1019.
49. Fortune B, Burgoyne CF, Cull GA, Reynaud J, Wang L. Structural and functional abnormalities of retinal ganglion cells measured in vivo at the onset of optic nerve head surface change in experimental glaucoma. *Invest Ophthalmol Vis Sci*. 2012;53:3939–3950.
50. Fujii H, Nohira K, Yamamoto Y, Ikawa H, Hjura T. Evaluation of blood flow by laser speckle image sensing, part 1. *Appl Opt*. 1987;26:5321–5325.
51. Sugiyama T, Araie M, Riva CE, Schmetterer L, Orgul S. Use of laser speckle flowgraphy in ocular blood flow research. *Acta Ophthalmol*. 2010;88:723–729.
52. Takahashi H, Sugiyama T, Tokushige H, et al. Comparison of CCD-equipped laser speckle flowgraphy with hydrogen gas

clearance method in the measurement of optic nerve head microcirculation in rabbits. *Exp Eye Res*. 2013;108:10–15.

53. Weinstein JM, Duckrow RB, Beard D, Brennan RW. Regional optic nerve blood flow and its autoregulation. *Invest Ophthalmol Vis Sci*. 1983;24:1559–1565.
54. Sossi N, Anderson DR. Effect of elevated intraocular pressure on blood flow. Occurrence in cat optic nerve head studied with iodoantipyrine I^{125}. *Arch Ophthalmol*. 1983;101:98–101.
55. Geijer C, Bill A. Effects of raised intraocular pressure on retinal, prelaminar, laminar, and retrolaminar optic nerve blood flow in monkeys. *Invest Ophthalmol Vis Sci*. 1979;18:1030–1042.
56. Garhofer G, Resch H, Weigert G, Lung S, Simader C, Schmetterer L. Short-term increase of intraocular pressure does not alter the response of retinal and optic nerve head blood flow to flicker stimulation. *Invest Ophthalmol Vis Sci*. 2005;46:1721–1725.
57. Riva CE, Hero M, Titze P, Petrig B. Autoregulation of human optic nerve head blood flow in response to acute changes in ocular perfusion pressure. *Graefes Arch Clin Exp Ophthalmol*. 1997;235:618–626.
58. Boltz A, Schmidl D, Werkmeister RM, et al. Regulation of optic nerve head blood flow during combined changes in intraocular pressure and arterial blood pressure. *J Cereb Blood Flow Metab*. 2013;33:1850–1856.
59. Schmidl D, Boltz A, Kaya S, et al. Comparison of choroidal and optic nerve head blood flow regulation during changes in ocular perfusion pressure. *Invest Ophthalmol Vis Sci*. 2012;53:4337–4346.
60. Schmidl D, Boltz A, Kaya S, et al. Role of nitric oxide in optic nerve head blood flow regulation during an experimental increase in intraocular pressure in healthy humans. *Exp Eye Res*. 2013;116C:247–253.
61. Movaffaghy A, Chamot SR, Petrig BL, Riva CE. Blood flow in the human optic nerve head during isometric exercise. *Exp Eye Res*. 1998;67:561–568.
62. Cull G, Burgoyne CF, Fortune B, Wang L. Longitudinal hemodynamic changes within the optic nerve head in experimental glaucoma. *Invest Ophthalmol Vis Sci*. 2013;54:4271–4277.
63. Berisha F, Feke GT, Hirose T, McMeel JW, Pasquale LR. Retinal blood flow and nerve fiber layer measurements in early-stage open-angle glaucoma. *Am J Ophthalmol*. 2008;146:466–472.
64. Rosengarten B, Hecht M, Kaps M. Brain activity affects dynamic but not static autoregulation. *Exp Neurol*. 2007;205:201–206.
65. Dawson SL, Blake MJ, Panerai RB, Potter JF. Dynamic but not static cerebral autoregulation is impaired in acute ischaemic stroke. *Cerebrovasc Dis*. 2000;10:126–132.
66. Peterson EC, Tozer K, Cohen W, Lam AM, Chesnut RM. Rethinking autoregulation in traumatic brain injury: a majority of patients with disruptive dynamic autoregulation do not respond to an elevated cerebral perfusion pressure. *Neurosurgery*. 2012;71:E560.
67. Guyton AC, Hall JE. *Textbook of Medical Physiology*. 11th ed. Philadelphia: Elsevier, Inc.; 2006; 173.

Investigative Ophthalmology & Visual Science